TDHB-splines: The Truncated Decoupled Basis of Hierarchical Tensor-product Splines

Dominik Mokriš[a,*], Bert Jüttler[a]

[a]*Institute of Applied Geometry, Johannes Kepler University of Linz, Altenberger Str. 69, 4040 Linz, Austria*

Abstract

We introduce a novel basis for multivariate hierarchical tensor-product spline spaces. Our construction combines the truncation mechanism (Giannelli et al., 2012) with the idea of decoupling basis functions (Mokriš et al., 2014). While the first mechanism ensures the partition of unity property, which is essential for geometric modeling applications, the idea of decoupling allows us to obtain a richer set of basis functions than previous approaches. Consequently, we can guarantee the completeness property of the novel basis for large classes of multi-level spline spaces. In particular, completeness is obtained for the multi-level spline spaces defined on T-meshes for hierarchical splines of (multi-) degree $\mathbf{p}$ for example (i) with single knots and $\mathbf{p}$-adic refinement and (ii) with knots of multiplicity $\mathbf{m} \geq (\mathbf{p}+\mathbb{1})/3$ and dyadic refinement (where each cell to be refined is subdivided into 2^d cells, with d being the number of variables) without any further restriction on the mesh configuration. Both classes (i,ii) include multivariate quadratic hierarchical tensor-splines with dyadic refinement.

Keywords: Hierarchical B-splines, box-mesh, T-mesh, dimension of splines, completeness, truncation, decoupling

1. Introduction

A subdivision of a domain in d-dimensional space into axis-aligned boxes is called a *box-mesh*, in particular a *T-mesh* for dimension $d = 2$. The analysis of the dimensions and the construction of bases of multivariate (with focus on bivariate) spline spaces on box meshes and T-meshes has been the topic of a substantial number of publications.

*Corresponding author. Tel. +43(0)732 2468 4080

Email addresses: dominik.mokris@jku.at (Dominik Mokriš), bert.juettler@jku.at (Bert Jüttler)

One of the earliest publications (Chui and Wang, 1983) included not only the dimension formula for splines on simple cross-cut grid partitions but also a detailed study on bivariate splines with rectangular grid partitions. More recently, Deng et al. (2006) proposed a method based on Bézier nets to calculate the dimension of a spline function space over a T-mesh, in particular in the case when the order of smoothness is less than half the degree of the spline functions, which corresponds to knot multiplicities satisfying $\mathbf{m} \geq (\mathbf{p} + \mathbb{1})/2$. We will refer to this class of functions – that allows to decouple the degrees of freedom – as *splines with reduced smoothness*.

The dimension of bivariate splines with reduced smoothness was reconsidered by Huang et al. (2006a), who derived an equivalent dimension formula using the smoothing cofactor method. A further extension was presented by Huang et al. (2006b). The dimension of trivariate splines on hierarchical box meshes for the case of reduced smoothness was investigated by Li et al. (2006b). Considering again the bivariate case, Li et al. (2006a) used the method of smoothing cofactors to derive a dimension formula for splines with reduced smoothness.

The splines of reduced smoothness have been used for surface modeling and reconstruction by Li et al. (2007) and Deng et al. (2008), where they were called PHT splines (Polynomial splines over Hierarchical T-meshes). See also Li et al. (2009) for the bicubic splines on general T-meshes. The extension to surfaces of arbitrary topology (i.e., including vertices of arbitrary valency) has been presented by Li et al. (2010). Wang et al. (2011) described the generalization to the case of piecewise rational functions and presented an application to numerical simulation using the novel approach of isogeometric analysis (cf. Cottrell et al., 2009). Isogeometric analysis with PHT splines was also studied by Nguyen-Thanh et al. (2011). Schumaker and Wang (2012) studied the approximation power of polynomial splines on T-meshes. This includes PHT splines as a special case. Also the dimension formula from Deng et al. (2006) and Huang et al. (2006b) is confirmed there.

In the general case (i.e., non-reduced smoothness), Li and Chen (2011) and Berdinsky et al. (2012) observed that the dimension of the spline space may depend on the geometry of the T-mesh. Mourrain (2014) presented a general approach based on homological algebra to analyze the dimension of bivariate splines on T-meshes. The resulting formula includes certain correction terms that are difficult to evaluate in general. For a special class of meshes, which are called diagonalizable T-meshes, Li (2012) provided a general dimension result that depends only on the topology of the T-mesh but not on its geometry. Wu et al. (2013) studied another special class of T-meshes and used Mourrain's approach to obtain a dimension formula. Wu et al. (2012) proposed a method for the construction of hierarchical bases of a bivariate spline space with the highest order smoothness over a consistent

hierarchical T-mesh. Deng et al. (2013) investigated the dimension of bivariate biquadratic spline spaces over T-meshes.

In these publications, the analysis of the spline space was performed independently on a specific construction of a basis (or, more generally, of a generating system). There exist three additional approaches, which start from the construction of a basis (or a generating system). These approaches are T-splines (see Scott et al. (2012) and the references cited therein), LR splines (Dokken et al., 2013) and hierarchical B-splines. We are interested in the latter approach, in particular we will consider the *completeness question:* Given a basis of a spline space, does the space spanned by it include all piecewise polynomial functions of the given degree and smoothness on the underlying T-mesh or box-mesh?

The construction of hierarchical splines was introduced by Forsey and Bartels (1988). About ten years later, Kraft (1997) presented a construction of a basis for this space. The completeness question for hierarchical B-splines was first investigated by Giannelli and Jüttler (2013) for bivariate splines of maximal smoothness. Meanwhile, these results have been extended to the trivariate case and to the case of non-uniform degrees and lower smoothness (Berdinsky et al., 2013, 2014a). A basis for bivariate spline spaces with maximal smoothness has been presented by Berdinsky et al. (2014b).

We summarize the development and the dependencies between some of these contributions in Figure 1. The arrows indicate the citations, where we omitted arrows that can be replaced by compositions of other arrows in order to keep the graph as simple as possible.

The present paper introduces a novel basis for multivariate hierarchical tensor-product spline spaces. Our construction combines the truncation mechanism (Giannelli et al., 2012) with the idea of decoupling the basis functions (Mokriš et al., 2014). Since the truncation mechanism may produce linearly dependent systems of functions, we use the novel framework for the truncation developed by Zore and Jüttler (2014) that applies to generating systems also. Moreover, we employ recent results on completeness obtained by Mokriš et al. (2014) and use them to characterize the completeness of the new basis.

The truncation mechanism ensures the partition of unity property, which is essential for geometric modeling applications. Using decoupling allows us to obtain a richer set of basis functions. Consequently we can guarantee the completeness property for large classes of multi-level spline spaces.

The remainder of this paper consists of five sections. First we introduce the notation and recall the notion of the multi-level spline space on the box mesh that is determined by a construction of hierarchical B-splines. Then we introduce decoupled splines, which form a new generating system for the spline functions on a multi-cell domain. Section 4 invokes the framework of Zore and Jüttler

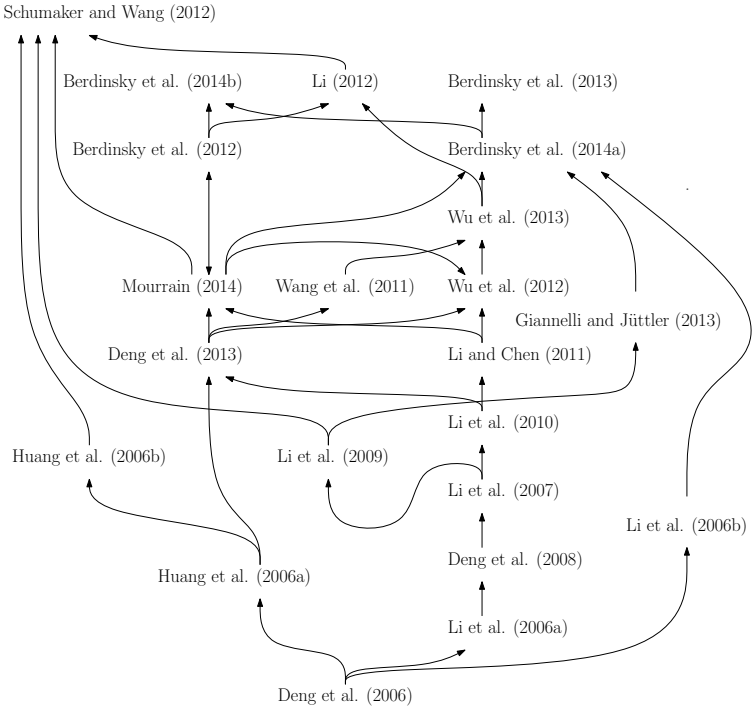

Figure 1: Selected papers and their dependencies (according to the citations).

(2014) in order to obtain the basis of truncated decoupled hierarchical B-splines (TDHB-splines), which forms a nonnegative partition of unity. The following section identifies conditions that guarantee the completeness of TDHB splines. Finally, we conclude the paper.

2. Preliminaries

We consider hierarchies of tensor-product spline functions defined on the d–dimensional space $\mathbb{R}^d$ with coordinates $\mathbf{x} = (x_1, \ldots, x_d)$. Given a number of levels N, we assume that a strictly increasing bi-infinite sequence of *(grid) nodes*

$$\left(g_{i,j}^{\ell}\right)_{j\in\mathbb{Z}}, \quad g_{i,j}^{\ell} < g_{i,j+1}^{\ell}$$

is given for each coordinate x_i, $i = 1, \ldots, d$ and for each level $\ell = 0, \ldots, N$. We require that these sequences are nested, i.e., $\left(g_{i,j}^{\ell}\right)_{j\in\mathbb{Z}}$ is a subsequence of $\left(g_{i,j}^{\ell+1}\right)_{j\in\mathbb{Z}}$. These nodes define *grid hyperplanes* of level ℓ,

$$\{\mathbf{x} \in \mathbb{R}^d \,|\, x_i = g_{i,j}^{\ell}\} \quad (i = 1, \ldots, d;\ j \in \mathbb{Z})$$

that form the *grid* of level ℓ. Figure 2 illustrates these notions by a bivariate example.

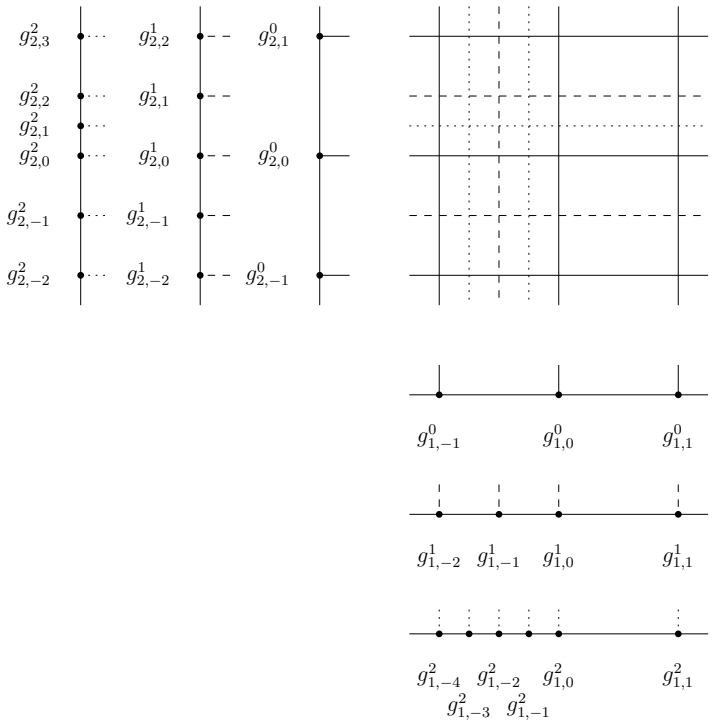

Figure 2: Nodes and grid hyperplanes for $d = 2$ and $N = 2$.

The grid nodes $g^\ell_{i,j}$ and the grid hyperplanes defined by them have associated multiplicities. In principle, these multiplicities could depend on the level ℓ, the index of the coordinate direction i and on the index j in the sequence of nodes. In order to keep the notation simple, we shall assume that the multiplicities are independent of j. Consequently, we denote them by $\mathbf{m}^\ell = (m^\ell_1, \ldots, m^\ell_d)$. However, most of the results presented in the remainder of the paper can be generalized to the case of non-uniform multiplicities.

The grid hyperplanes subdivide the d–dimensional space $\mathbb{R}^d$ into *cells of level* ℓ,

$$c^\ell_{\mathbf{j}} = \bigtimes_{i=1}^{d} [g^\ell_{i,j_i-1}, g^\ell_{i,j_i}],$$

where X denotes simply the Cartesian product and $\mathbf{j} = (j_1, \ldots, j_d) \in \mathbb{Z}^d$. Let $\mathcal{C}^\ell$ be the set of all cells of level ℓ. Any union of finitely many cells from $\mathcal{C}^\ell$ will be called a *multi-cell domain of level* ℓ.

Let Ω be a bounded open domain in $\mathbb{R}^d$ and consider open sets Ω^ℓ, $\ell = 0, \ldots, N+1$ satisfying

$$\Omega = \Omega^0 \supseteq \Omega^1 \supseteq \cdots \supseteq \Omega^{N+1} = \emptyset.$$

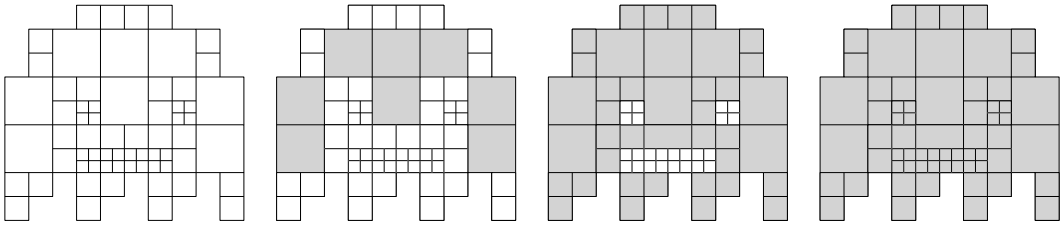

(a) mesh (b) ring Δ^0 (c) ring Δ^1 (d) ring Δ^2

Figure 3: An example of a hierarchical mesh and the associated rings.

This nested sequence of open domains will be called the *domain hierarchy*. In addition, we will consider the complementary hierarchy of the so-called *rings*

$$\Delta^\ell = \overline{\Omega^0 \setminus \Omega^{\ell+1}} \quad (\ell = 0, \dots, N),$$

which satisfy $\Delta^\ell \subseteq \Delta^{\ell+1}$. The following assumption will be essential:

(A1) Each Δ^ℓ is a multi-cell domain of level ℓ, i.e., a union of cells of level k with $k \leq \ell$.

An example is shown in Figure 3.

In order to define a *hierarchy of spline spaces*, we consider a sequence of (multi-) degrees $\mathbf{p}^\ell = (p_1^\ell, \dots, p_d^\ell)$ and multiplicities $\mathbf{m}^\ell = (m_1^\ell, \dots, m_d^\ell)$ that are assumed to satisfy

(A2) $1 \leq m_i^\ell \leq p_i^\ell, \quad p_i^{\ell+1} - p_i^\ell \leq m_i^{\ell+1} - m_i^\ell,$ and $p_i^\ell \leq p_i^{\ell+1}$.

For each level ℓ and each coordinate direction x_i we use the nodes $g_{i,j}^\ell$ and the associated multiplicities m_i^ℓ to define a bi-infinite knot sequence, simply by repeating each node m_i^ℓ times. Further we denote with B_i^ℓ the basis of B-splines with variable x_i that are defined on these knot sequences. More precisely, each tuple of $p_i^\ell + 2$ adjacent knots defines a B-spline, e.g., by the well-known B-spline recurrence formula (see Prautzsch et al., 2002). The collection of these B-splines forms the basis B_i^ℓ. The knot multiplicities do not exceed the degrees, hence all B-splines are continuous.

For each level ℓ we denote with $\bigotimes_{i=1}^d B_i^\ell$ the set of tensor-product B-splines that are obtained by multiplying d univariate B-splines, one from each B_i^ℓ. Moreover, we collect the tensor-product B-splines that are not equal to the null function on Ω,

$$\{\gamma^\ell \in \bigotimes_{i=1}^d B_i^\ell \mid \gamma^\ell|_\Omega \neq 0\}.$$

In the remainder of the paper we will consider only the restrictions of these B-splines to Ω and denote them simply by γ_i^ℓ. They form the (tensor-product) *B-spline basis vector*

$$\mathbf{G}^\ell = (\gamma_1^\ell, \ldots, \gamma_{n^\ell}^\ell)^T$$

and we denote its size by n^ℓ (note that ℓ is an upper index, not a power). The elements of this vector span the space

$$\mathbb{V}^\ell = \operatorname{span} \mathbf{G}^\ell|_\Omega.$$

The assumption (A2) concerning degrees and multiplicities together with the nestedness of the sequences of grid nodes imply that these spaces are nested, $\mathbb{V}^\ell \subseteq \mathbb{V}^{\ell+1}$. Furthermore, there exist *refinement matrices* $\mathbf{R}^\ell = (r_{ij}^\ell)$ such that

$$\mathbf{G}^\ell = \mathbf{R}^{\ell+1}\mathbf{G}^{\ell+1} \quad (\ell = 0, \ldots, N). \tag{1}$$

These matrices can be generated with the help of the knot insertion algorithm for B-splines, see Prautzsch et al. (2002). Due to the linear independence and the partition of unity property of tensor-product B-splines, these matrices are *left stochastic*[1], i.e., all their entries are nonnegative and the column vectors sum to one. Indeed, Eq. (1) combined with

$$1 = \mathbb{1}^\ell \mathbf{G}^\ell = \mathbb{1}^{\ell+1}\mathbf{G}^{\ell+1} \tag{2}$$

implies $\mathbb{1}^\ell \mathbf{R}^{\ell+1} = \mathbb{1}^{\ell+1}$, where $\mathbb{1}^k$ denotes the row vector of dimension n^k with all its elements being equal to 1.

Given an open set $D \subset \mathbb{R}^d$, we denote with $\Pi^{\mathbf{p}}(\overline{D})$ the linear space of multivariate polynomials of degree $\mathbf{p}$ on its closure $\overline{D}$ and with $C^{\mathbf{s}}(\overline{D})$ the linear space of all functions with the property that all their partial derivatives up to order $\mathbf{s} = (s_1, \ldots, s_d)$ exist at all points of D and they can be continuously extended to the closure $\overline{D}$.

Definition 1. For each ring Δ^ℓ we define the *spline space* of level ℓ,

$$\mathbb{S}^\ell = \{s : \Delta^\ell \to \mathbb{R} \mid s \in C^{\mathbf{p}^\ell - \mathbf{m}^\ell}(\Delta^\ell) \text{ and } \forall c \in \mathcal{C}^\ell, c \subseteq \Delta^\ell : s|_c \in \Pi^{\mathbf{p}^\ell}(c)\}.$$

Further, we define the *multi-level spline space*

$$\mathbb{S} = \{s : \Omega \to \mathbb{R} \mid \forall_{\ell=0}^N : \ s|_{\Delta^\ell} \in \mathbb{S}^\ell\}.$$

The remainder of this paper discusses the construction and some properties of a basis for the multi-level spline space under certain assumptions concerning the domain hierarchy.

[1]Here we extend the notion *left stochastic* to non-square matrices. Products of left stochastic matrices are again left stochastic.

3. Decoupled splines

We enrich the B-spline bases by introducing a decoupling mechanism. This mechanism will allow us to split the B-splines in $\mathbf{G}^\ell$ into several independent components according to the connectivity of the intersection of their support with the corresponding ring Δ^ℓ.

We consider the *support* of functions defined on Ω,

$$\operatorname{supp} f = \{\mathbf{x} \in \overline{\Omega} \,|\, f(\mathbf{x}) \neq 0\}. \tag{3}$$

Given a function $\gamma_i^\ell \in \mathbf{G}^\ell$, we consider its representation with respect to the basis functions of the next level,

$$\gamma_i^\ell = \sum_{j=1}^{n^{\ell+1}} r_{ij}^{\ell+1} \gamma_j^{\ell+1} = \mathbf{r}_i^{\ell+1} \mathbf{G}^{\ell+1}. \tag{4}$$

The coefficient vector in this equation is the i-th row vector of the refinement matrix $\mathbf{R}^{\ell+1}$ in Eq. (1). The *decoupling graph* Γ_i^ℓ is defined as follows:

- The basis functions $\gamma_j^{\ell+1}$ with nonzero coefficients $r_{ij}^{\ell+1} \neq 0$ are *vertices* of Γ_i^ℓ.
- Two vertices $\gamma_j^{\ell+1}$ and $\gamma_{j'}^{\ell+1}$ are connected by an *edge* if and only if

$$\operatorname{supp} \gamma_j^{\ell+1} \cap \operatorname{supp} \gamma_{j'}^{\ell+1} \cap \Delta^\ell \neq \emptyset.$$

Further we denote by Ξ_i^ℓ the set of all connected components of Γ_i^ℓ (which is a set of graphs) and we use the symbol ε to denote the relation "is a vertex of". For example, $\gamma \,\varepsilon\, \Phi$ means that γ is a vertex of the graph Φ.

Figure 4 shows a decoupling graph of a quintic B-spline with uniform knots. In this example, the graph has 7 vertices, 7 edges and three connected components. Uniform dyadic refinement splits the the quintic B-splines into 7 finer ones, thus the graph has 7 vertices. The supports of the first four finer B-splines (green dashed lines) mutually intersect each other within Δ^0, hence the corresponding vertices are connected by edges and form a connected component of the graph. Similarly, the supports of the last two finer B-splines (blue and dashed) intersect each other within Δ^0, hence the corresponding vertices are connected by edges and form another connected component of the graph. The remaining finer B-spline (red) corresponds to an isolated vertex of the decoupling graph. See also Example 3.

Definition 2. We define the *decoupled B-splines* $\delta_{i,\Phi}^\ell$ of level ℓ by

$$\delta_{i,\Phi}^\ell = \sum_{\substack{j=1,\dots,n^{\ell+1} \\ \gamma_j^{\ell+1} \,\varepsilon\, \Phi}} r_{ij}^{\ell+1} \gamma_j^{\ell+1} \quad (\ell = 0, \dots, N;\ i = 1, \dots, n^\ell;\ \Phi \in \Xi_i^\ell). \tag{5}$$

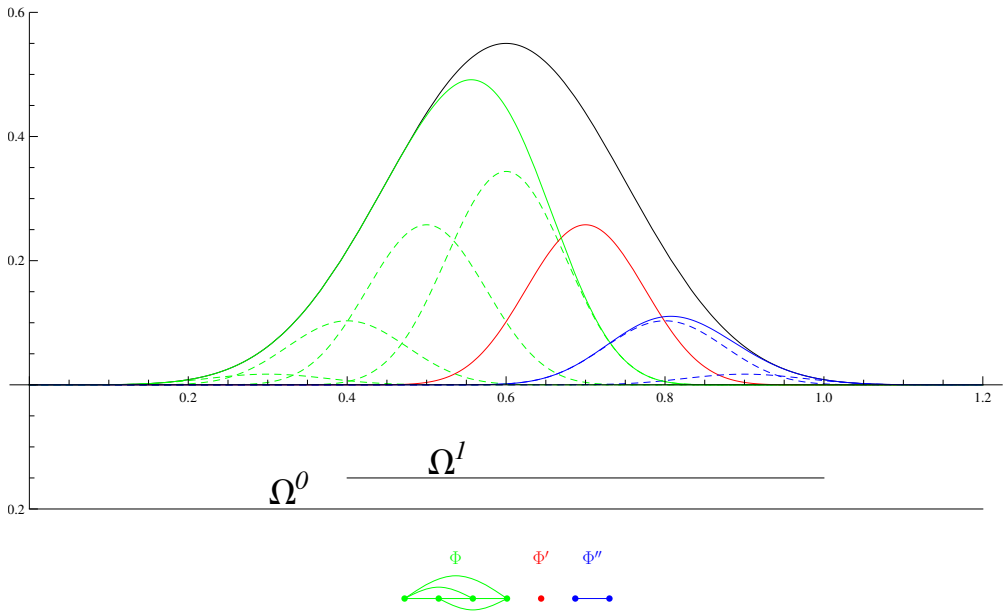

Figure 4: Top: Quintic B-spline (black) of level 0 and decoupled B-splines (green, red and blue) derived from it by choosing $\Omega^1 = (0.4, 1)$. The decoupled B-splines are sums of B-splines from the finer level (dashed). Bottom: Associated decoupling graph.

A similar definition was presented in Mokriš et al. (2014). However, we did not consider the isolated vertices of the decoupling graph there.

Each of the B-splines of level ℓ is split into one or more decoupled B-splines, one for each connected component of the decoupling graph. Each decoupled B-spline is a linear combination of B-splines of level $\ell + 1$, with coefficients inherited from the B-spline refinement equation. Note that the decoupled B-splines are not necessarily different from each other. In particular, each B-spline $\gamma_j^{\ell+1}$ of level $\ell+1$ with $\operatorname{supp} \gamma_j^{\ell+1} \cap \Delta^\ell = \emptyset$, which is therefore an isolated vertex of the decoupling graphs, may be present as a decoupled B-spline several times.

Example 3. Figure 4 shows the decoupling graph and the decoupled B-splines which are obtained from a single quintic B-spline of degree 5 with uniform knots $(\ldots, -0.2, 0, 0.2, \ldots)$ and dyadic refinement. Choosing the domain $\Omega^1 = (0.4, 1)$ leads to three decoupled B-splines.

In order to describe the relation between B-splines and decoupled B-splines in detail, we collect the decoupled B-splines of level ℓ in a column vector

$$\hat{\mathbf{G}}^\ell = (\hat{\gamma}_1^\ell, \ldots, \hat{\gamma}_{\hat{n}^\ell}^\ell)^T$$

of dimension

$$\hat{n}^\ell = \sum_{i=1}^{n^\ell} |\Xi_i^\ell|.$$

Here $|\Xi_i^\ell|$ denotes the number of elements of the set Ξ_i^ℓ, i.e., the number of connected components of the decoupling graph Γ_i^ℓ.

Each of the functions $\delta_{i,\Phi}^\ell$ from Definition 2 defines exactly one element of the vector $\hat{\mathbf{G}}^\ell$,

$$\hat{\gamma}_{k(i,\Phi)}^\ell = \delta_{i,\Phi}^\ell,$$

where the index $k = k(i, \Phi)$ is determined by the index i of the original B-spline γ_i^ℓ and by the connected component Φ of the decoupling graph. A suitable ordering of $\hat{\mathbf{G}}^\ell$ will be suggested in the next section.

Example 4. It is possible that the decoupled B-splines $\hat{\mathbf{G}}^\ell$ are linearly dependent. As an example, we consider bi-quartic B-splines with single knots on a uniform grid and dyadic refinement. Figure 5 shows two functions (top left and top right; both represented by their supports). The refined grid has been omitted. For both functions, the decoupling graph consists of two connected components that possess edges and a number of isolated vertices (see Figure 6). The supports of the decoupled functions obtained from the first two components are shown in the center of the top row and in the bottom row, left and right. The isolated vertices of both graphs produce 16 decoupled B-splines, which are the same (though scaled differently) for both functions; the union of their supports is shown in the center of the bottom row. Consequently, $\hat{\mathbf{G}}^\ell$ is linearly dependent.

The refinement equation between B-splines and decoupled B-splines,

$$\mathbf{G}^\ell = \mathbf{D}^\ell \hat{\mathbf{G}}^\ell, \tag{6}$$

can be formulated with the help of a left stochastic matrix $\mathbf{D}^\ell$,

$$\mathbb{1}^\ell \mathbf{D}^\ell = \hat{\mathbb{1}}^\ell, \tag{7}$$

where $\mathbb{1}^\ell$ and $\hat{\mathbb{1}}^\ell$ denote the row vectors of dimensions n^ℓ and $\hat{n}^\ell$, respectively, with all elements equal to 1. Indeed, since any B-spline is split into a sum of decoupled B-splines, all entries of this matrix are zero except for one entry per column, which is equal to 1.

The refinement equation between the decoupled B-splines and the B-splines of the next finer level takes the form

$$\hat{\mathbf{G}}^\ell = \mathbf{X}^{\ell+1} \mathbf{G}^{\ell+1}. \tag{8}$$

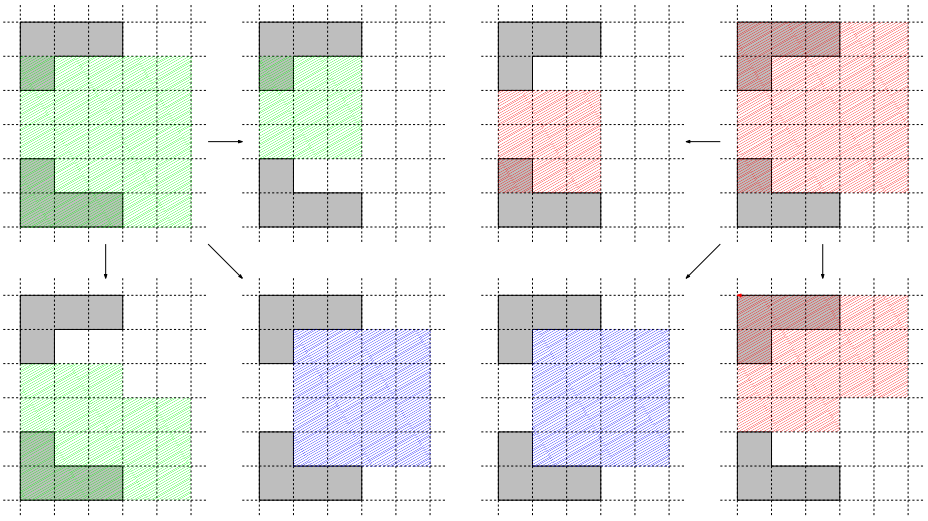

Figure 5: Decoupling bi-quartic B-splines with single knots and dyadic refinement. The ring Δ^ℓ is shown in gray. The hatched regions are supports of functions from $\mathbf{G}^\ell$ and $\hat{\mathbf{G}}^\ell$, the arrows show the decoupling. The two functions in the top left and top right are decoupled into 2 larger functions and 16 B-splines (corresponding to isolated vertices of the coefficient graph) each.

where $\mathbf{X}^{\ell+1}$ is a left stochastic matrix. Equations (2), (6) and (7) give

$$1 = \mathbb{1}^\ell \mathbf{G}^\ell = \mathbb{1}^\ell \mathbf{D}^\ell \hat{\mathbf{G}}^\ell = \hat{\mathbb{1}}^\ell \hat{\mathbf{G}}^\ell = \hat{\mathbb{1}}^\ell \mathbf{X}^{\ell+1} \mathbf{G}^{\ell+1} = \mathbb{1}^{\ell+1} \mathbf{G}^{\ell+1},$$

hence we conclude by comparing the coefficients that $\hat{\mathbb{1}}^\ell \mathbf{X}^{\ell+1} = \mathbb{1}^{\ell+1}$, as the elements of $\mathbf{G}^{\ell+1}$ are linearly independent. In fact, the entries of each row of the refinement matrix in Eq. (1) are distributed into several rows of the matrix $\mathbf{X}^{\ell+1}$, one for each connected component of the decoupling graph.

The next lemma summarizes several properties of decoupled B-splines.

Lemma 5. *We consider the decoupled B-splines $\hat{\mathbf{G}}^\ell$ of level ℓ.*

(i) The sum of the decoupled B-splines derived from a B-spline is the B-spline itself,

$$\sum_{\Phi \in \Xi_i^\ell} \delta_{i,\Phi}^\ell = \gamma_i^\ell.$$

In particular, if $\operatorname{supp} \gamma_i^\ell \subseteq \Delta^\ell$, then γ_i^ℓ decouples into exactly one function $\delta_{i,\Phi}^\ell = \gamma_i^\ell$.

(ii) If $\Phi \neq \Phi'$, then

$$\operatorname{supp} \delta_{i,\Phi} \cap \operatorname{supp} \delta_{i,\Phi'} \cap \Delta^\ell = \emptyset.$$

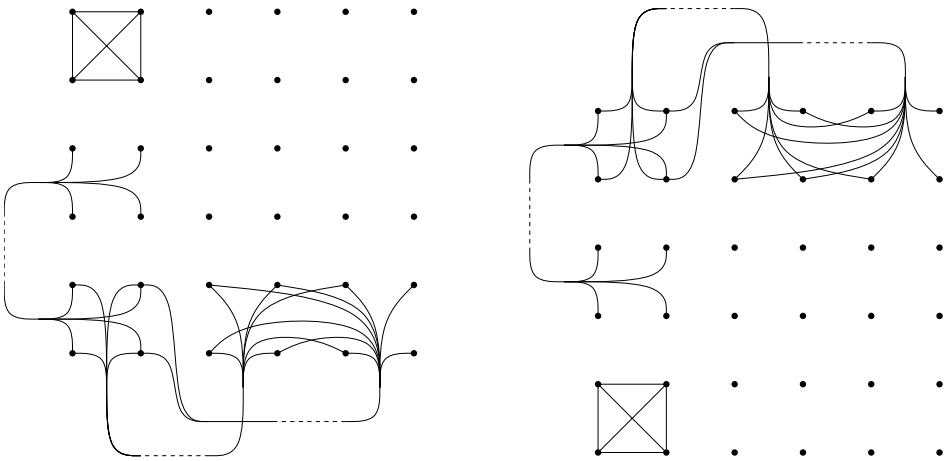

Figure 6: The decoupling graphs of the functions from Figure 5.

(iii) The decoupled B-splines possess the property of local linear independence on Δ^ℓ. *More precisely, for any open set* $D \subset \Delta^\ell$,

$$0|_D = \sum_{j=1}^{\hat{n}^\ell} \xi_j \, \hat{\gamma}_j^\ell|_D \quad \Rightarrow \quad \forall\, j = 0, \dots, \hat{n}^\ell : \; \xi_j = 0 \;\vee\; \operatorname{supp} \hat{\gamma}_j^\ell \cap D = \emptyset.$$

Proof. The first two properties follow directly from Definition 2. In order to prove the third observation, we note that the decoupled B-splines form a decomposition of each B-spline into several functions with disjoint supports on Δ^ℓ. Since the B-splines possess the property of local linear independence, this is also true for the decoupled B-splines on Δ^ℓ. □

Note that the local linear independence of $\hat{\mathbf{G}}^\ell$ on Δ^ℓ does not imply its linear independence on Ω, cf. Example 4.

Proposition 6. *The decoupled B-splines form a nonnegative partition of unity,*

$$1 = \sum_{i=0}^{\hat{n}^\ell} \hat{\gamma}_i^\ell \quad \textit{and} \quad \forall \mathbf{x} \in \Omega : \; \hat{\gamma}_i^\ell(\mathbf{x}) \geq 0$$

Proof. Since the matrix $\mathbf{X}^{\ell+1}$ is left stochastic, we get

$$\hat{\mathbb{1}}^\ell \mathbf{X}^{\ell+1} = \mathbb{1}^{\ell+1}.$$

The B-splines of level $\ell + 1$ form a nonnegative partition of unity,

$$\mathbb{1}^{\ell+1} \mathbf{G}^{\ell+1} = 1.$$

The proof can be completed by combining both observations. □

Proposition 7. *The vectors of decoupled B-splines satisfy the refinement equations*

$$\hat{\mathbf{G}}^\ell = \hat{\mathbf{R}}^{\ell+1}\hat{\mathbf{G}}^{\ell+1} \quad (\ell = 0, \dots, N-1),$$

where all matrices $\hat{\mathbf{R}}^{\ell+1}$ *are left stochastic.*

Proof. Equations (6) and (8) imply

$$\hat{\mathbf{R}}^{\ell+1} = \mathbf{X}^{\ell+1}\mathbf{D}^{\ell+1}.$$

The product of two left stochastic matrices is again left stochastic. □

Example 8. In case of biquadratic splines with dyadic refinement and single knots each basis function from $\mathbf{G}^\ell$ has a support consisting of 3×3 cells. The possible shapes of the supports of decoupled functions are shown in Figure 7 (up to rotations and symmetries). An example of a mesh with all these basis functions is shown in Figure 8.

4. (Truncated) Hierarchical decoupled splines

We define hierarchical and truncated hierarchical decoupled splines. Our construction generalizes the results of Kraft (1997) and Giannelli et al. (2012). However, since the systems of decoupled B-splines are not guaranteed to be linearly independent, we use the approach that was developed in Zore and Jüttler (2014).

This approach is based on the observation that we may split each of the vectors $\hat{\mathbf{G}}^\ell$ of decoupled B-splines into three sub-vectors $\hat{\mathbf{G}}^\ell_A$, $\hat{\mathbf{G}}^\ell_B$ and $\hat{\mathbf{G}}^\ell_C$,

$$\hat{\mathbf{G}}^\ell = \begin{pmatrix} \gamma^\ell_1 \\ \vdots \\ \gamma^\ell_{\hat{n}^\ell} \end{pmatrix} = \begin{pmatrix} \hat{\mathbf{G}}^\ell_A \\ \hat{\mathbf{G}}^\ell_B \\ \hat{\mathbf{G}}^\ell_C \end{pmatrix} \tag{9}$$

such that

$$\begin{aligned} &\gamma^\ell_i \text{ is an element of } \hat{\mathbf{G}}^\ell_A \Leftrightarrow \operatorname{supp} \gamma^\ell_i \not\subseteq \Omega^\ell, \\ &\gamma^\ell_i \text{ is an element of } \hat{\mathbf{G}}^\ell_C \Leftrightarrow \operatorname{supp} \gamma^\ell_i \subseteq \Omega^{\ell+1}, \\ &\gamma^\ell_i \text{ is an element of } \hat{\mathbf{G}}^\ell_B \text{ otherwise.} \end{aligned}$$

More precisely, we assume that the order of the decoupled B-splines within the vectors $\hat{\mathbf{G}}^\ell$ has been chosen so that this splitting into sub-vectors becomes feasible.

Clearly, the three sub-vectors have mutually different entries, since the domains Ω^ℓ are assumed to be nested. Also, it should be noted that not all sub-vectors are present at all levels. For instance, both $\hat{\mathbf{G}}^0_A$ and $\hat{\mathbf{G}}^N_C$ are void.

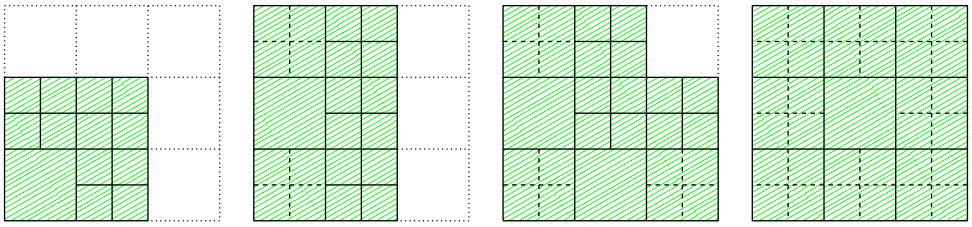

Figure 7: Possible shapes of supports of decoupled biquadratic spline functions, up to rotations and symmetries, depending on the local shape of the mesh in the support. Here we assume that there are no intersections with the boundary of the domain Ω. The larger cells belong to level ℓ, whereas the smaller ones to level $\ell + 1$. The dotted lines indicate the size of the support before decoupling, whereas the dashed lines may or may not be present as long as the mesh does not reduce to a case with a smaller support. Note that due to (3) the supports near to domain boundary are possibly trimmed, see Figure 8.

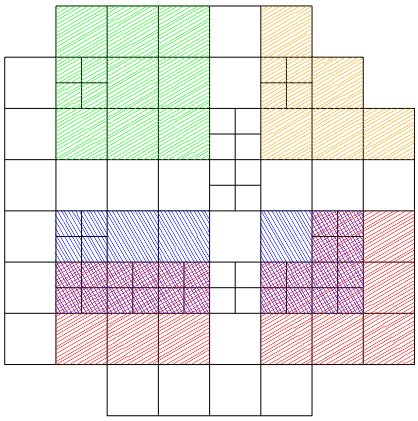

Figure 8: Mesh with biquadratic decoupled B-splines. The support of a basis function (provided that it is sufficiently far away from the boundary of Ω) consists of 3×3 cells. The function may split into up to 4 decoupled functions. In the example, the functions either split into two functions (pairs of red and blue supports with purple overlap) or remain unchanged (green supports). The shape of the support of the upper right function (orange) is caused by the intersection with the domain boundary.

The elements of the two sub-vectors $\hat{\mathbf{G}}_A^\ell$ and $\hat{\mathbf{G}}_B^\ell$ are linearly independent. This is due to the fact that $\hat{\mathbf{G}}^\ell$ possesses the property of local linear independence on Δ^ℓ (see Lemma 5 (iii)) and these two subvectors contain exactly the decoupled B-splines that do not vanish on Δ^ℓ.

The refinement equation from Proposition 7 can now be formulated with a

matrix consisting of 3×3 blocks,

$$\hat{\mathbf{G}}^\ell = \begin{pmatrix} \hat{\mathbf{G}}^\ell_A \\ \hat{\mathbf{G}}^\ell_B \\ \hat{\mathbf{G}}^\ell_C \end{pmatrix} = \begin{pmatrix} \mathbf{R}^{\ell+1}_{AA} & \mathbf{R}^{\ell+1}_{AB} & \mathbf{R}^{\ell+1}_{AC} \\ \mathbf{R}^{\ell+1}_{BA} & \mathbf{R}^{\ell+1}_{BB} & \mathbf{R}^{\ell+1}_{BC} \\ \mathbf{0} & \mathbf{R}^{\ell+1}_{CB} & \mathbf{R}^{\ell+1}_{CC} \end{pmatrix} \begin{pmatrix} \hat{\mathbf{G}}^{\ell+1}_A \\ \hat{\mathbf{G}}^{\ell+1}_B \\ \hat{\mathbf{G}}^{\ell+1}_C \end{pmatrix} = \mathbf{R}^{\ell+1} \hat{\mathbf{G}}^{\ell+1}. \tag{10}$$

The lower left block-matrix is a null matrix $\mathbf{0}$, since $\mathbf{R}^{\ell+1}$ has nonnegative entries, the decoupled B-splines are nonnegative, and $\operatorname{supp} \hat{\mathbf{G}}^\ell_C \subseteq \Omega^{\ell+1}$.

Definition 9. We define the *decoupled hierarchical B-splines*

$$\mathcal{K} = (\hat{\mathbf{G}}^\ell_B)_{\ell=0}^N$$

and the *truncated decoupled hierarchical B-splines*

$$\mathcal{T} = \left(\hat{\mathbf{T}}^\ell\right)_{\ell=0}^N,$$

where

$$\hat{\mathbf{T}}^\ell = \mathbf{R}^{\ell+1}_{BA} \left(\prod_{k=\ell+2}^{N} \mathbf{R}^k_{AA} \right) \hat{\mathbf{G}}^N_A \quad (\ell = 0, \ldots, N-1)$$

and $\hat{\mathbf{T}}^N = \hat{\mathbf{G}}^N_B$.

The following results have been derived in the general setting, see Zore and Jüttler (2014):

- The two systems of functions $\mathcal{K}$ and $\mathcal{T}$ have the same number of elements and they span the same space.
- When restricted to Δ^ℓ, the functions in $\hat{\mathbf{G}}^\ell_B$ and $\hat{\mathbf{T}}^\ell$ are identical,

$$\hat{\mathbf{G}}^\ell_B|_{\Delta^\ell} = \hat{\mathbf{T}}^\ell|_{\Delta^\ell}.$$

- Both $\mathcal{K}$ and $\mathcal{T}$ are linearly independent. This follows directly from the fact that the decoupled B-splines $\hat{\mathbf{G}}^\ell$ possess the property of local linear independence on Δ^ℓ, see Lemma 5 (iii).
- The truncated decoupled hierarchical B-splines form a nonnegative partition of unity,

$$\sum_{\ell=0}^{N} \sum_{i=1}^{\hat{n}^\ell_B} \hat{\tau}^\ell_i = 1 \quad \text{and} \quad \text{all } \hat{\tau}^\ell_i \geq 0 \text{ on } \Omega,$$

  where $\hat{\mathbf{T}}^\ell = (\hat{\tau}^\ell_1, \ldots, \hat{\tau}^\ell_{\hat{n}^\ell_B})^T$ and $\hat{n}^\ell_B$ is the size of $\hat{\mathbf{G}}^\ell_B$. This fact is implied by Proposition 6.

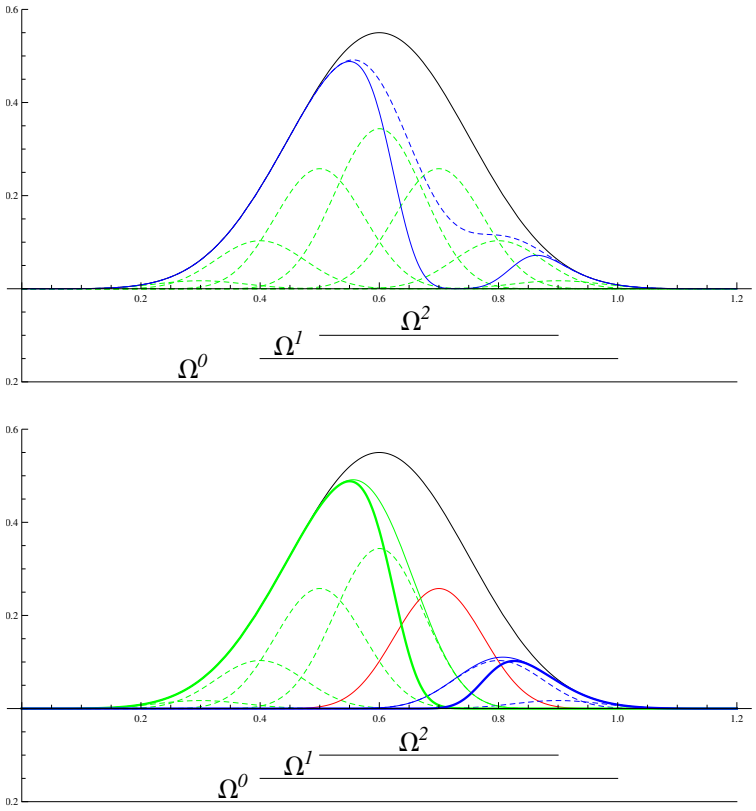

Figure 9: Functions obtained by applying truncation (top) and decoupling with truncation (bottom) to the quintic B-spline from Example 3 for a domain hierarchy with three levels. Using only truncation leads to a single truncated function (solid blue), while decoupling and truncation gives two functions (thick blue and thick green).

Example 10. We continue Example 3 and compare the effects of truncation and decoupling in Figure 9. First we apply only truncation, thus we obtain only one function. The upper picture shows the functions obtained after truncation with respect to level 1 (blue, dashed) and after truncation with respect to both levels 1 and 2 (blue, solid). The bottom picture shows the corresponding decoupled functions.

5. Completeness of (T)DHB-splines

We identify conditions that guarantee the completeness of (truncated) decoupled hierarchical B-splines, i.e., conditions that allow to represent any piecewise polynomial function of the given degree and smoothness on the hierarchical grid

determined by the hierarchies of spaces and domains. First we recall a result from Mokriš et al. (2014):

Proposition 11. *Consider the sets* $\operatorname{supp}\delta \cap \Delta^\ell$*, where* δ *is any element of* $\hat{\mathbf{G}}_A^\ell$ *or* $\hat{\mathbf{G}}_B^\ell$*. If all these sets are connected, then the elements of the two vectors* $\hat{\mathbf{G}}_A^\ell$ *and* $\hat{\mathbf{G}}_B^\ell$ *form a basis of the spline space* $\mathbb{S}^\ell$*.*

Proof. Consider the decoupled basis functions that are derived from a given B-spline γ. When restricted to Δ^ℓ, these functions have mutually disjoint supports. On each connected component of $\operatorname{supp}\gamma \cap \Delta^\ell$, exactly one of them is equal to the B-spline γ, while the remaining functions vanish identically. These properties are implied by Lemma 5 (i) and (ii). Consequently, each of the decoupled B-splines from $\hat{\mathbf{G}}_A^\ell$ or $\hat{\mathbf{G}}_B^\ell$, restricted to Δ^ℓ, is equal to exactly one of the functions that form the basis described in (Mokriš et al., 2014, Theorem 2.12). □

Note that a ring Δ^ℓ may contain kissing edges, kissing vertices, etc. If such a kissing feature is contained in the support of a decoupled function, then the intersection of the support with Δ^ℓ is connected across that feature, since Δ^ℓ is a closed set.

Now we formulate the main result of the paper.

Theorem 12. *If the assumptions of Proposition 11 are satisfied for all* $\ell = 0, \ldots, N$*, then each of the systems* $\mathcal{K}$ *and* $\mathcal{T}$ *forms a basis of* $\mathbb{S}$*. Moreover,* $\mathcal{T}$ *is a nonnegative partition of unity.*

Proof. The proof is fairly similar to the proof of Theorem 20 in Giannelli and Jüttler (2013). Nevertheless, since there are a few subtle differences and in order to make this paper self-contained, we repeat it here in a compact form.

We consider a function $s \in \mathbb{S}$. We will show that there exist $N+1$ functions

$$s^\ell \in \operatorname{span}\begin{pmatrix}\hat{\mathbf{G}}_A^\ell \\ \hat{\mathbf{G}}_B^\ell\end{pmatrix} \quad (\ell = 0, \ldots, N) \tag{11}$$

such that

$$s^\ell|_{\Delta^\ell} = \left(s - \sum_{i=0}^{\ell-1} s^i\right)\Big|_{\Delta^\ell}, \tag{12}$$

using induction with respect to ℓ.

For $\ell = 0$ this follows directly from Proposition 11 and from the definition of $\mathbb{S}$. According to the latter, $s \in \mathbb{S}$ implies $s|_{\Delta^0} \in \mathbb{S}^0$. Recall that $\hat{\mathbf{G}}_A^0$ is void. Now, in order to proceed from $\ell - 1$ to ℓ, we first prove that the right-hand side of Equation (12) belongs to $\mathbb{S}^\ell$. Once again, according to the definition of $\mathbb{S}$, $s \in \mathbb{S}$ implies $s|_{\Delta^\ell} \in \mathbb{S}^\ell$. Consequently, Proposition 11 guarantees that $s|_{\Delta^\ell}$ can be

represented by a linear combination of functions from $\hat{\mathbf{G}}_A^\ell$ and $\hat{\mathbf{G}}_B^\ell$. In addition, since

$$s^k \in \operatorname{span} \begin{pmatrix} \hat{\mathbf{G}}_A^k \\ \hat{\mathbf{G}}_B^k \end{pmatrix} \quad (k = 0, \dots, \ell - 1)$$

there exist row vectors $\mathbf{c}^k$ such that

$$s^k = \mathbf{c}^k \hat{\mathbf{G}}^k = \mathbf{c}^k \hat{\mathbf{R}}^{k+1} \hat{\mathbf{G}}^{k+1} = \cdots = \mathbf{c}^k \prod_{j=k+1}^{N} \hat{\mathbf{R}}^j \hat{\mathbf{G}}^\ell.$$

Here we used the refinement equations (7) in order to express each s^k with respect to the decoupled B-splines of level ℓ. The definition of the sub-vectors in (9) now implies that

$$s^k|_{\Delta^\ell} \in \operatorname{span} \begin{pmatrix} \hat{\mathbf{G}}_A^\ell \\ \hat{\mathbf{G}}_B^\ell \end{pmatrix} |_{\Delta^\ell} \quad (k = 0, \dots, \ell - 1).$$

Thus, we can find s^ℓ satisfying (11) and (12). This completes the induction step.

Analyzing the right-hand side of equation (12) confirms that $s^\ell|_{\Delta^{\ell-1}} = 0$. Therefore, the local linear independence of the decoupled B-splines (Lemma 5 (ii)) and the definition of the sub-vectors in (9) imply that the coefficients with respect to $\hat{\mathbf{G}}_A^\ell$ are zero, and thus $s^\ell \in \operatorname{span} \hat{\mathbf{G}}_B^\ell$.

Finally, if we rewrite (12) for $\ell = N$, we obtain

$$s = s|_{\Delta^N} = \sum_{\ell=0}^{N} s^\ell|_{\Delta^N},$$

which proves that $\mathcal{K} = (\hat{\mathbf{G}}_B^\ell)_{\ell=0}^N$ spans $\mathbb{S}$. Both $\mathcal{K}$ and $\mathcal{T}$ are known to be linearly independent and to span the same space, see Section 4. Moreover $\mathcal{T}$ is known to be a nonnegative partition of unity. □

One of the motivations for introducing the decoupled basis is to relax the assumptions on the rings Δ^ℓ that are sufficient to guarantee the completeness of $\mathcal{K}$ and $\mathcal{T}$. More precisely, we obtain the following result.

Theorem 13. *A sufficient condition for the assumption of Proposition 11 to be satisfied is that none of the basis functions from the finer level (i.e., from $\mathbf{G}^{\ell+1}$) intersects Δ^ℓ in more than one connected set.*

Proof. The proof follows immediately from the fact that the support of each decoupled B-spline from $\hat{\mathbf{G}}_A^\ell \cup \hat{\mathbf{G}}_B^\ell$ is the union of supports of B-splines from the next level that are vertices of one connected component of the decoupling graph obtained for one B-spline of level ℓ, see Lemma 5 (i). □

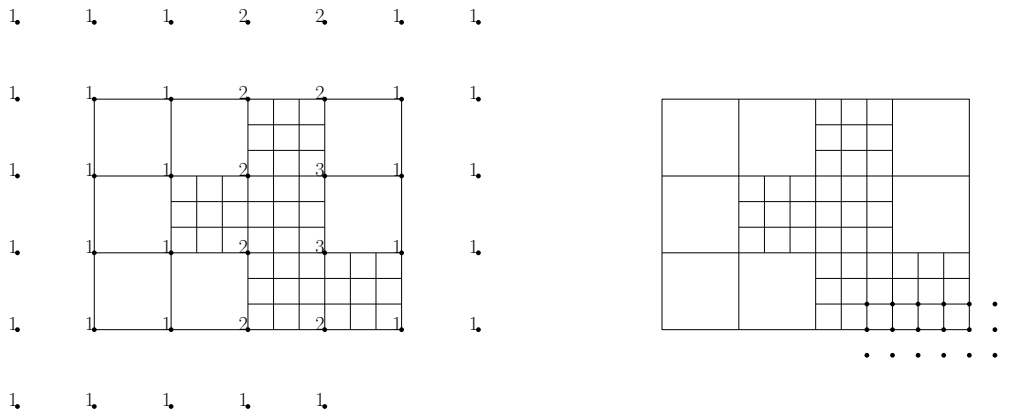

Figure 10: Bicubic B-splines from $\mathbf{G}_B^0$ and $\mathbf{G}_B^1$. Left: dots are placed in the Greville points corresponding to functions from $\mathbf{G}_B^0$ and the labels specify the number of functions from $\hat{\mathbf{G}}_B^0$ the particular function decouples into. Right: functions from $\mathbf{G}_B^1$.

Now we are going to discuss several cases where this assumption is satisfied.

Corollary 14. *Suppose that the degrees are independent of the level, $\mathbf{p}^\ell = \mathbf{p}$, and all knots possess multiplicity 1. When using $\mathbf{p}$-adic refinement (i.e., each cell of level ℓ is split into $p_1 \times \cdots \times p_d$ cells of level $\ell + 1$), the basis $\mathcal{T}$ spans the entire space $\mathbb{S}$ and this basis forms a nonnegative partition of unity.*

Proof. Under this assumption, the support of each function from $\mathbf{G}^{\ell+1}$ is contained in $(p_1 + 1) \times \cdots \times (p_d + 1)$ cells of level $\ell + 1$. This guarantees that its intersection with Δ^ℓ is always connected and the claim follows from Theorem 13. Alternatively, we may notice that the support of each function from $\hat{\mathbf{G}}^\ell$ is contained in $2 \times \cdots \times 2$ cells of level ℓ and refer directly to Theorem 12. □

An example is shown in Figure 10.

The following corollary relaxes the assumption $2\mathbf{m}^\ell \geq \mathbf{p}^\ell + \mathbb{1}$, $\mathbb{1} = (1, \ldots, 1)^T$, characterizing the case of reduced smoothness that is considered frequently in the literature, e.g., by Deng et al. (2006) or Schumaker and Wang (2012).

Corollary 15. *If the cells in level ℓ are refined by splitting them into 2^d cells of level $\ell + 1$ (dyadic refinement) and the multiplicities satisfy*

$$3\mathbf{m}^\ell \geq \mathbf{p}^\ell + \mathbb{1},$$

then $\mathcal{T}$ is a basis of $\mathbb{S}$ and it forms a nonnegative partition of unity.

Proof. Under this assumption concerning knot multiplicities, the support of each function from $\mathbf{G}^{\ell+1}$ is contained in $3 \times \cdots \times 3$ cells of level $\ell + 1$. This implies that its intersection with Δ^ℓ is always connected and we may again use Theorem 13. □

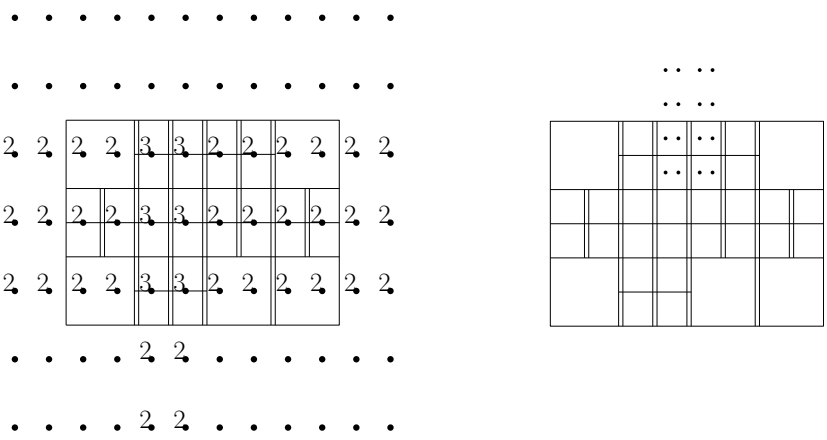

Figure 11: Bivariate B-splines with $\mathbf{p}^\ell = (5, 4)$ and $\mathbf{m}^\ell = (2, 1)$. Left: dots depict the Greville points functions from $\mathbf{G}_B^0$; those that decouple into more than one function have a label indicating the number of decoupled functions derived from them. Right: B-splines from $\mathbf{G}_B^1$, which are also present in $\mathcal{T}$.

See Figure 11 for an example.

Remark 16. Note that both results are valid for any dimension, but they apply only to box-meshes that are obtained by **p**-adic / dyadic refinement. More general configurations have also been studied in the literature, mostly in the bivariate case. We mention the recent results on bivariate splines on more general T-meshes (but with slightly lower smoothness) by Schumaker and Wang (2012). This analysis also includes results concerning the approximation power and the stability properties.

Finally we consider the case of maximum smoothness and uniform degrees.

Corollary 17. *Consider the case $d = 2$ or $d = 3$ with dyadic refinement, uniform degrees $\mathbf{p}^\ell = (p, \dots, p)$ and uniform knots of multiplicity 1 at all levels. If the offsets for all distances up to $\frac{p-1}{4}$ with respect to the grid size of level ℓ (that is, the offsets for all distances up to $\frac{p-1}{2}$ with respect to the gridsize of the finer mesh) of each ring Δ^ℓ do not have any self-intersections, then $\mathcal{T}$ is a basis of $\mathbb{S}$ and forms a nonnegative partition of unity.*

Here we consider the offset with respect to the maximum norm. We refer to Mokriš et al. (2014) for the precise definition. Figure 12 shows an example for $d = 2$.

Remark 18. Multivariate quadratic $C^{\mathbf{1}}$–smooth splines on meshes with dyadic refinement (where each box is refined into 2^d smaller boxes) are covered by all three corollaries. The offset condition from Corollary 17 is then automatically fulfilled.

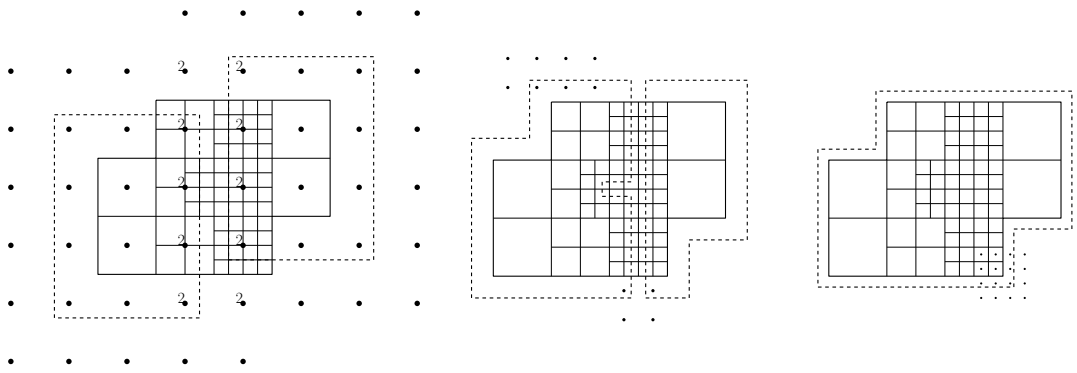

Figure 12: Multi-level mesh with bi-quartic basis functions. The dashed lines represent the offsets at distance 3/4. From left to right: TDHB-splines from $\hat{\mathbf{G}}_B^0, \hat{\mathbf{G}}_B^1, \hat{\mathbf{G}}_B^2$. Note that the offset condition would not be satisfied for larger degrees.

Interestingly, not all the edges (or, more generally, interfaces between adjacent edges) are necessarily being used by some of the basis functions. Figure 13 shows an example of a T-mesh with "passive" edges.

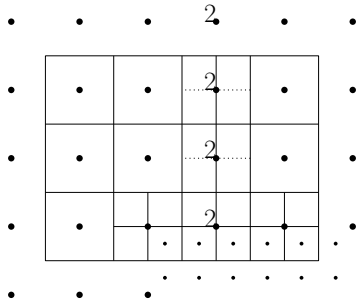

Figure 13: Biquadratic splines. Thick dots correspond to Greville points from $\mathbf{G}_B^0$, the smaller dots to functions from $\mathbf{G}_B^1$. If a number is present at a dot, it specifies the number of functions that this function decouples into (note that the functions from the finest level do not get decoupled). The dotted lines represent the "passive" edges, i.e., the edges that could be omitted without changing the dimension of the spline space.

6. Conclusions and future work

We presented the construction of truncated decoupled hierarchical B-splines. It generalizes the classical hierarchical construction and it keeps some of the desirable properties of B-splines (e.g., linear independence, nonnegative partition of unity) while simultaneously providing a richer set of basis functions.

Further work may include investigation of approximation properties of this basis, derivation of an explicit dimension formula and practical applications in Isogeometric Analysis and Geometric Modeling.

Acknowledgements. The authors have been supported by the Austrian Science Fund (FWF), NFN S117 "Geometry + Simulation" and by the EC through the 7th Framework programme, project EXAMPLE, GA no. 324340.

References

Berdinsky, D., Kim, T.-W., Bracco, C., Cho, D., Mourrain, B., Oh, M., Kiatpanichgij, S., 2014a. Dimensions and bases of hierarchical tensor-product splines. J. Comput. Appl. Math. 257, 86–104.

Berdinsky, D., Kim, T.-W., Bracco, C., Cho, D., Oh, M., Seo, Y., 2014b. Iterative refinement of hierarchical T-meshes for bases of spline spaces with highest order smoothness. Comput. Aided Design 47, 96–107.

Berdinsky, D., Kim, T.-W., Cho, D., Bracco, C., 2013. Bases of T-meshes and the refinement of hierarchical B-splines, https://sites.google.com/site/berdinsky/.

Berdinsky, D., Oh, M., Kim, T.-W., Mourrain, B., 2012. On the problem of instability in the dimension of a spline space over a T-mesh. Computers & Graphics 36 (5), 507–513.

Chui, C. K., Wang, R. H., 1983. On smooth multivariate spline functions. Math. Comp. 41 (163), 131–142.

Cottrell, J. A., Hughes, T. J. R., Bazilevs, Y., 2009. Isogeometric Analysis: Toward Integration of CAD and FEA. John Wiley & Sons.

Deng, J., Chen, F., Feng, Y., 2006. Dimensions of spline spaces over T–meshes. J. Comput. Appl. Math. 194, 267–283.

Deng, J., Chen, F., Jin, L., 2013. Dimensions of biquadratic spline spaces over T-meshes. J. Comput. Appl. Math. 238, 68–94.

Deng, J., Chen, F., Li, X., Hu, C., Tong, W., Yang, Z., Feng, Y., 2008. Polynomial splines over hierarchical T-meshes. Graph. Models 70, 76–86.

Dokken, T., Lyche, T., Pettersen, K. F., 2013. Polynomial splines over locally refined box–partitions. Comput. Aided Geom. Design 30, 331–356.

Forsey, D. R., Bartels, R. H., 1988. Hierarchical B-spline refinement. Comput. Graphics 22, 205–212.

Giannelli, C., Jüttler, B., 2013. Bases and dimensions of bivariate hierarchical tensor–product splines. J. Comput. Appl. Math. 239, 162–178.

Giannelli, C., Jüttler, B., Speleers, H., 2012. THB–splines: the truncated basis for hierarchical splines. Comput. Aided Geom. Design 29, 485–498.

Huang, Z., Deng, J., Feng, Y., Chen, F., 2006a. New proof of dimension formula of spline spaces over T-meshes via smoothing cofactors. J. Comput. Math. 24 (4), 501–514.

Huang, Z., Deng, J., Li, X., Feng, Y., 2006b. Dimensions of spline spaces over general T-meshes. Journal of University of Science and Technology of China 36 (6), 573–581.

Kraft, R., 1997. Adaptive and linearly independent multilevel B–splines. In: Le Méhauté, A., Rabut, C., Schumaker, L. L. (Eds.), Surface Fitting and Multiresolution Methods. Vanderbilt University Press, Nashville, pp. 209–218.

Li, C.-J., Wang, R.-H., Zhang, F., 2006a. Improvement on the dimensions of spline spaces on T-mesh. J. of Information & Computational Science 3 (2), 235–244.

Li, X., 2012. On the dimension of splines spaces over T-meshes with smoothing cofactor-conformality method. arXiv preprint 1210.5312.

Li, X., Chen, F., 2011. On the instability in the dimension of splines spaces over T-meshes. Comput. Aided Geom. Design 28 (7), 420–426.

Li, X., Deng, J., Chen, F., 2006b. Dimensions of spline spaces over 3D hierarchical T-meshes. J. of Information & Computational Science 3, 487–501.

Li, X., Deng, J., Chen, F., 2007. Surface modeling with polynomial splines over hierarchical T-meshes. Visual Comput. 23, 1027–1033.

Li, X., Deng, J., Chen, F., 2009. C1 bicubic splines over general T-meshes. In: Proc. Conference on CAD/Graphics. IEEE, pp. 92–95.

Li, X., Deng, J., Chen, F., 2010. Polynomial splines over general T-meshes. Visual Comput. 26 (4), 277–286.

Mokriš, D., Jüttler, B., Giannelli, C., 2014. On the completeness of hierarchical tensor-product B-splines. J. Comput. Appl. Math. 271, 53–70.

Mourrain, B., 2014. On the dimension of spline spaces on planar T–meshes. Math. Comp. 83 (286), 847–871.

Nguyen-Thanh, N., Nguyen-Xuan, H., Bordas, S., Rabczuk, T., 2011. Isogeometric analysis using polynomial splines over hierarchical T-meshes for two-dimensional elastic solids. Comput. Meth. Appl. Mech. Engrg. 200, 1892–1908.

Prautzsch, H., Boehm, W., Paluszny, M., 2002. Bézier and B–spline Techniques. Springer.

Schumaker, L. L., Wang, L., 2012. Approximation power of polynomial splines on T–meshes. Comput. Aided Geom. Design 29, 599–612.

Scott, M. A., Li, X., Sederberg, T. W., Hughes, T. J. R., 2012. Local refinement of analysis-suitable T-splines. Computer Methods in Applied Mechanics and Engineering 213–216, 206–222.

Wang, P., Xu, J., Deng, J., Chen, F., 2011. Adaptive isogeometric analysis using rational PHT-splines. Computer-Aided Design 43 (11), 1438–1448.

Wu, M., Deng, J., Chen, F., 2013. Dimension of spline spaces with highest order smoothness over hierarchical T-meshes. Comput. Aided Geom. Design 30 (1), 20–34.

Wu, M., Xu, J., Wang, R., Yang, Z., 2012. Hierarchical bases of spline spaces with highest order smoothness over hierarchical T–subdivisions. Comput. Aided Geom. Design 29, 499–509.

Zore, U., Jüttler, B., 2014. Adaptively refined multilevel spline spaces from generating systems. Comp. Aided Geom. Design, to appear.